View metadata, citation and similar papers at core.ac.uk
brought to you by CORE
provided by Aberdeen University Research Archive

PCCP

ARTICLE TYPE

Cite this: DOI: 10.1039/xxxxxxxxxx

A comprehensive study of the thermal conductivity of the hard sphere fluid and solid by Molecular Dynamics simulation

Sławomir Pieprzyk,[a] Arkadiusz C. Brańka,[a] David M. Heyes[b] and Marcus N. Bannerman[c]

Received Date
Accepted Date

DOI: 10.1039/xxxxxxxxxx

www.rsc.org/journalname

This work reports a new set of hard sphere (HS) thermal conductivity coefficient, λ, data obtained by Molecular Dynamics (MD) computer simulation, over a density range covering the dilute fluid to near the close-packed solid, and for a large number of particles (up to $N = 131072$) and long simulation times. The $N-$dependence of the thermal conductivity is shown to be proportional to $N^{-2/3}$ to a good approximation over a wide range of system sizes, which enabled λ values in the thermodynamic limit to be predicted accurately. The fluid and solid λ can be represented well by the Enskog theory (ET) formula, λ_E, times a density-dependent correction term, which is close to unity for the fluid and practically constant for the solid. The convergence of the MD λ data back towards ET in the metastable fluid starts just above the freezing density. For the HS solid and dense fluid it was found that the thermal conductivity is nearly linear in pressure, as has been observed experimentally for a number of solids. Simple excess entropy scaling over the higher density fluid phase region was found, and Rosenfeld's exponential relationship can be fitted to the simulation data for the solid to a high degree of accuracy. The simulation analysis has revealed a number of new trends in the behaviour of the HS thermal conductivity which could be useful in building more accurate models for heat conduction in experimental systems.

1 Introduction

The hard sphere (HS) potential and type of particle has been widely used over many decades as a reference model for different fluid and solid systems of practical interest. The HS system is defined with the pairwise interaction

$$u(r) = \begin{cases} \infty, & 0 < r < \sigma, \\ 0, & r > \sigma, \end{cases} \tag{1}$$

where r is the interparticle separation and σ is the sphere diameter. Its simplicity has enabled approximate semi-empirical analytic formulae for many physical properties to be derived, with the aid of Molecular Dynamics (MD) and Monte Carlo simulations, which compare favourably with experiment.[1,2] Compared to equation of state and structural characterisations (mainly using the radial distribution function) there have been relatively few systematic studies with MD of the transport coefficients of the HS system over a wide density range since the pioneering MD study of Alder, Gass and Wainright[3] in 1970 (see ref. 4 and 5 for more recent studies in the same vein). This is rather surprising as these quantities have proved important in interpreting the behaviour of a wide range of experimental systems. Thermal conduction has been found experimentally important for a diverse range of molecular and hard particle systems, for example, refrigerants,[6] granular,[7,8] and colloidal liquids (e.g., thermofluids[9]). The recent growth of research into nanofluids has also driven a reexamination of the underlying nature of thermal conduction in mixtures (e.g. ref. 10 and 11) and recent results have shown anomalous extrema in λ appear as a function of composition[12] for particular mixtures. The λ of single component and binary hard sphere mixtures,[13–15] provide useful reference models for these systems and thus a more accurate characterisation of the density dependence of the hard sphere thermal conductivity would therefore seem timely.

In our previous publication[16] we carried out an MD simulation investigation of the self-diffusion coefficient, D, and shear viscosity, η_s, of the HS fluid. This is extended here to consider the thermal conductivity, λ. The HS thermal conductivity shows qualitative differences from the shear viscosity and self-diffusion coefficient. For example, there is no sharp change in its value in the freezing-melting transition region.

In this work the thermal conductivity of a single-component hard sphere fluid and solid is determined for a range of densities in the equilibrium fluid, metastable and solid states using MD. The λ values in the various density regions are fitted to semi-empirical

[a] Institute of Molecular Physics, Polish Academy of Sciences, M. Smoluchowskiego 17, 60-179 Poznań, Poland; E-mail: pieprzyk@ifmpan.poznan.pl, branka@ifmpan.poznan.pl
[b] Department of Physics, Royal Holloway, University of London, Egham, Surrey TW20 0EX, United Kingdom; E-mail: david.heyes@rhul.ac.uk
[c] School of Engineering, University of Aberdeen, AB24 3UE, United Kingdom; E-mail: m.campbellbannerman@abdn.ac.uk

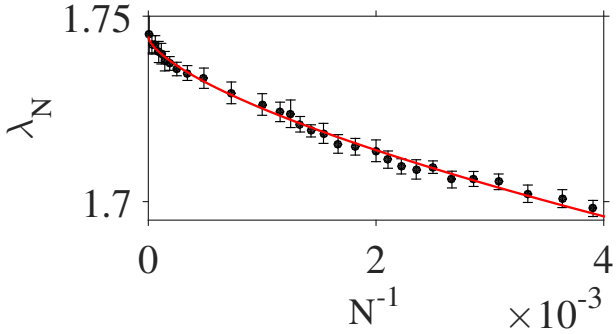

Fig. 1 The $N-$dependent thermal conductivity, λ_N, as a function of system size, N^{-1}, for one representative density, $\rho = 0.4$. The black solid points are the MD data for $N = 256$, 275, 300, 325, 350, 375, 400, 425, 450, 475, 500, 550, 600, 650, 700, 750, 800, 864, 1000 1372, 2048, 2916, 4000, 5324, 6912, 8788, 10976, 16384, 32000 and 131072 particles. The solid red line is an $N^{-2/3}$ fit to the MD data, which corresponds to the straight line in Fig. 2.

expressions, and a number of notable trends are discovered and discussed.

The work is organized as follows. In Sec. 2 the theory and calculation details of the thermal conductivity of the hard sphere system are covered. The thermal conductivity data and density-dependent trends are discussed for the equilibrium and metastable fluid in Sec. 3, and for the solid in Sec. 4. The main conclusions are summarised in Sec. 5.

2 Theory and calculation details

The computed thermal conductivity values are compared here with Enskog theory which is an extension of the kinetic theory of gas formulae for the transport coefficients to finite densities. It incorporates excluded volume effects but assumes the successive collisions between the molecules are uncorrelated. The Enskog formula for the thermal conductivity of the hard sphere fluid is,[17–19]

$$\lambda_E = \lambda_0 \rho b_2 \left[\frac{1}{\mathscr{Z}} + 1.2 + 0.7574 \mathscr{Z} \right]. \tag{2}$$

Its value in the limit of zero density, λ_0, from kinetic theory, is given by

$$\lambda_0 = 1.02513 \frac{75 k_B}{64 \sigma^2} \left(\frac{k_B T}{m \pi} \right)^{1/2}, \tag{3}$$

where the first term, 1.02513, is the Sonine polynomial correction factor up to the 4th term,[17] which is found widely in the literature, although the limiting value is 1.025218 but this makes no practical difference to the results.[20] In the above formulae, $b_2 = 2\pi\sigma^3/3$, is the second viral coefficient. The unit of time is $(m\sigma^2/k_B T)^{1/2}$, where m is the mass of the hard sphere particle, k_B is the Boltzmann constant and T is the temperature. The thermal conductivity coefficient is in $k_B \sigma^{-2} (k_B T/m)^{1/2}$ units. The only independent and key state variable is the hard sphere number density which, for N particles in volume, V, is defined as, $\rho = N/V$. For simplicity all reported quantities are expressed in terms of σ, m and T. The quantity $\mathscr{Z} = Z - 1$, where $Z = P/\rho k_B T$ is the compressibility factor, and P is the pressure. The three terms in Eq. (2) represent the kinetic (kk), cross (kc) and collisional (cc) contributions, respectively.

There are two well-established methods for determining the transport coefficients of model liquids by MD. These are the Green-Kubo (GK) time correlation function approach, and by rearrangement, the Einstein-Kubo-Helfand (EKH) method.[21]

A simulation-averaged time correlation function or mean square quantity, respectively, is evaluated from which the transport coefficient is determined by time integration and differentiation, in the two approaches, respectively. It has been found more convenient to use the EKH route for hard spheres, in part, because the contributions from the collisions are not obtained at fixed time intervals, in contrast to the case when MD is applied to continuous potential systems. This causes time resolution issues for the time correlation function, which can be minimised in the mean square approach as the long time limit is what is required there. The EKH approach is used here to obtain the thermal conductivity via[22,23]

$$L_{ii}(t) = \frac{1}{2tVk_B T^2} \left\langle [G_{ii}(t)]^2 \right\rangle_{t_0}, \tag{4}$$

where t is the correlation time, the index, i, refers to the x, y, z directions and the angular brackets $\langle \ldots \rangle_{t_0}$ denote an averaging over the time origins, t_0. The Helfand moment $G_{ij}(t)$ is defined as the microscopic heat flux over a number of collisions, c, which for the hard-sphere system has the form,

$$G_{ii}(t) = \sum_{(c-1,c)} \left(\sum_{a=1}^{N} \frac{p_{ai}}{m} e_a \right)_{(c-1,c)} \Delta t_{c-1,c} + \sum_c \Delta e_a^{(c)} r_{abi}^{(c)} \theta(t - t_c), \tag{5}$$

where, in the first term $\Delta t_{c-1,c}$ is the time between collisions, $(c-1)$ and c during which the momenta remain constant, and $\theta(t - t_c)$ is the Heaviside step function at the time t_c. $e_a = \sum_{i=1}^{3} p_{ai}^2/2m$, and $\Delta e_a^{(c)} = e_a^+ - e_a^-$ where $+$ and $-$ indicate 'after' and 'before' the collision, respectively. In the second term, a and b denote the particles interacting at the collision c and $r_{abi}^{(c)} = r_{ai}(t_c) - r_{bi}(t_c)$. The first sum runs over the intercollisional free flights while the second sum is over the collision sequence. Note that from Eq. (4) three contributions to the thermal conductivity are computed at each collision, which corresponds to energy transport in the x, y, and z-directions. Owing to the cubic symmetry of solid phase (the FCC crystal) the thermal conductivity is an isotropic quantity in the HS system, and averaging over the three values, can be used to improve the statistics, and the desired value is the following long-time limit, $\lambda = \lim_{t\to\infty}(L_{xx}(t) + L_{yy}(t) + L_{zz}(t))/3$. The values of the transport coefficients depend to various extents on the number of HS in the simulation cell, the density and the particular transport coefficient chosen. The $N-$dependence is an important issue which requires extensive analysis for different N values in order to estimate the transport coefficient values in the thermodynamic limit. For example, as determined in detail in ref. 16, the self-diffusion coefficient displays a considerable $N-$dependence. In contrast, the shear viscosity does not exhibit a significant $N-$dependence even for relatively small system sizes, and at not too high densities, whereas at high fluid densities the $N-$dependence of the shear viscosity of small systems can dis-

This journal is © The Royal Society of Chemistry [year]

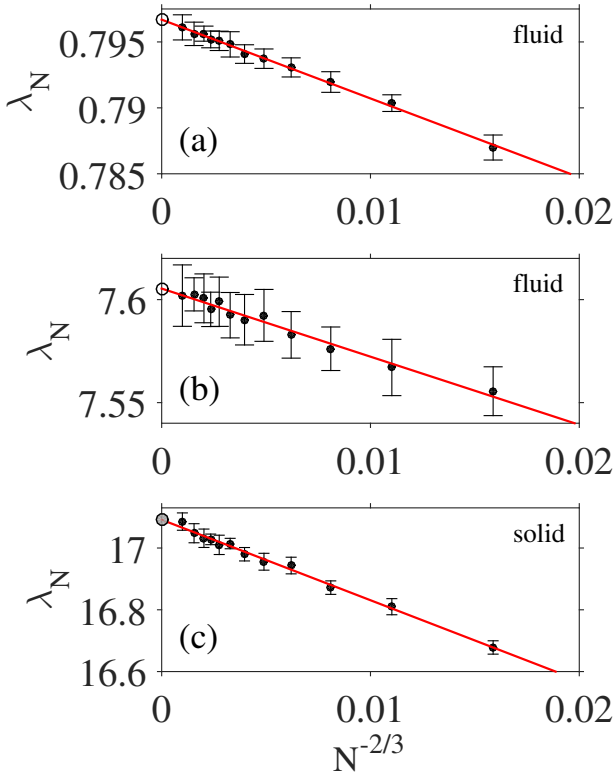

Fig. 2 The thermal conductivity λ_N as a function of system size, $N^{-2/3}$, for two fluid densities: (a) $\rho = 0.1$, (b) $\rho = 0.8$, and one solid density: (c) $\rho = 1.1$. The black solid points are the MD data for $N = 500$, 864, 1372, 2048, 2916, 4000, 5324, 6912, 8788, 10976, 16384, and 32000 particles. The red line is a linear fit to the MD data using Eq. (6). The black open and the grey solid circles represent, respectively, the thermal conductivity for fluid and solid HS systems in thermodynamic limit obtained from linear extrapolation (for $N > 1000$ particles).

play a quite complex-oscillatory behaviour.[24] In the case of the thermal conductivity it is hard to find any systematic study of the system size dependence in the literature. In this work, a comprehensive analysis of this issue has been performed, which has allowed a more accurate estimate of the thermodynamic limit values of λ compared to previous studies to be obtained.

For a range of different densities, from very dilute fluid to an almost close-packed crystal, extensive MD calculations were performed for systems containing $N = 500$, 864, 1372, 2048, 2916, 4000, 5324, 6912, 8788, 10976, 16384 and 32000 particles in the simulation cubic box. Additionally, for $\rho = 0.4$ the thermal conductivity was calculated for a system composed of $N = 131072$ particles to confirm the trend of the size dependence. The calculations were carried out with the DynamO MD program for event-driven systems involving discontinuous potentials.[25] In the simulations the system was equilibrated for 10^5 collisions per particle, and then production data were collected over the following 1.5×10^6 collisions per particle (which means 1.64×10^9 equilibrated collisions, and 2.46×10^{10} collisions in total in the case of $N = 16384$). Each simulation was conducted at least $10 - 20$ times to improve the statistics, and each density was started from different initial random velocities. Statistical errors in all simulation property averages were estimated by the block average method.[26] These calculations are very extensive in terms of the range of N considered and the length of the runs, which are several orders of magnitude longer than those of the previous studies cited here.

The resulting MD simulation data indicate that the functional form of the system size dependence of the HS thermal conductivity is more complex than just $1/N$. For each density the λ_N *vs.* N^{-1} dependence is shown in Fig. 1. The MD data cannot be approximated well by a straight line when plotted as a function of N^{-1}. The points systematically deviate from the line by bending upwards over a wide range of N. Additionally, for the fluid densities the calculations were performed for a number of system sizes $864 \geq N \geq 256$ to confirm the monotonic character of the size dependence of the thermal conductivity. The λ data from this work indicates that the size dependence of the HS thermal conductivity can be represented well by,

$$\lambda_\infty = \lambda_N + \frac{A}{N^{2/3}}, \tag{6}$$

where the density dependence of the correction factor is, $A = -0.90449\exp(2.2978\rho) - 1.0233 \cdot 10^{-11}\exp(27.809\rho)$ for the fluid and $A = -1.1703\exp(2.3063\rho) - 1.3189 \cdot 10^{-10}\exp(20.834\rho)$ for the solid state. The formula for A has no obvious physical significance and the MD data could possibly be fitted just as well be another analytic form. Note that the A formula Eq. (6) applies only to the total thermal conductivity. The kk, kc and cc components of A were difficult to obtain reliably, even with this very accurate data. The results in Table 1 and 2 for the total λ and its kk, kc and cc components were obtained as in Fig. 2 i.e., from the linear extrapolation with the $N^{-2/3}$ scaling. In the rest of this report the identity, $\lambda \equiv \lambda_\infty$, will be employed.

The dependence in Eq. (6) means the HS thermal conductivity converges with the increasing area of the simulation cell i.e., $\sim L^{-2}$, where $L \sim N^{1/3}$ is the sidelength of the simulation box. The $N^{-2/3}$ N-dependence may arise from the fact that the heat flux is an energy transfer per unit area quantity, and the area of each face of the simulation cell is proportional to $N^{2/3}$. This result enables us to compare the system size dependence of three of the HS transport coefficients. Combining the conclusions from ref. 16 we have found that, $D \sim L^{-1}$, $\lambda \sim L^{-2}$ and $\eta_s \sim L^{-3}$. Representative examples of the system size-dependence of the HS thermal conductivity are shown in Fig. 2. Note from the figure that even relatively small systems obey this dependence well. It was verified that for most densities systems with $256 < N < 864$ the linear λ_N dependence in $N^{-2/3}$ was followed.

3 Hard sphere fluid

In this section the results of an analysis of the thermal conductivity data for the HS fluid (including the metastable region) is presented. The λ and its three components (kk, kc, and cc) are shown in Fig. 3, and listed in Table 1.

Figure 4 compares the data values from Table 1 with Enskog theory and demonstrates that λ is well-represented by the Enskog formula given in Eq. (2). This has been observed before for λ (e.g., ref. 4). In contrast, for the other transport coefficients, it is well known that agreement with Enskog theory only occurs

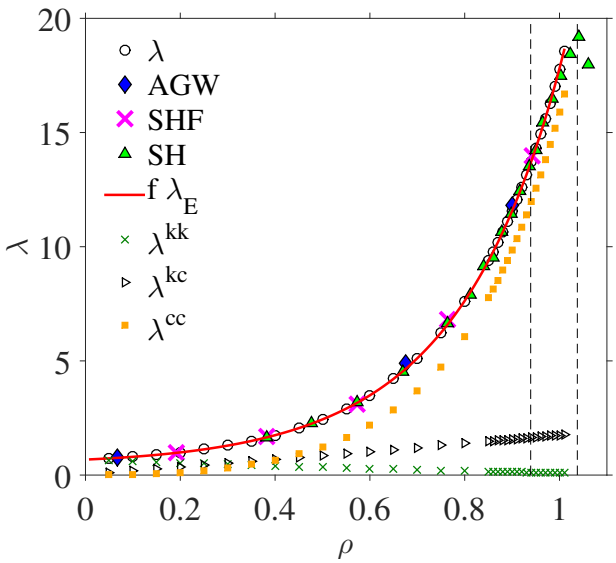

Fig. 3 Thermal conductivity and its components (kk, kc, cc) of hard sphere fluid. The black open circles are the results of this work (Table 1). The blue solid diamonds represent the results from Alder *et al.*[3] ($N = 500$) or 'AGW'. The magenta crosses are from Smith *et al.*[27] ($N = 500$) or 'SHF'. The green solid triangles are from Sigurgeirsson and Heyes[4] ($N = 4000$) or 'SH'. All of the sets of data were extrapolated to the thermodynamic limit with the scaling formula in Eq. (6). The green crosses, open right-triangles and orange solid squares are the kk, kc, cc components of λ (Table 1), respectively. The solid red line is Eq. (7). The vertical thin dashed lines indicate the freezing and melting densities.

at very low densities. This similarity is often exploited in representing the transport coefficient as the product of the Enskog formula and a density dependent function determined by MD. For the thermal conductivity the λ_E is multiplied by a polynomial function, f,

$$\lambda = f\lambda_E. \tag{7}$$

A 5th order polynomial, $f = \sum^5 d_n\rho^n$, with the coefficients $d_0 = 1$, $d_1 = 0.182181$, $d_2 = -0.487068$, $d_3 = 0.301668$, $d_4 = 0.450921$, and $d_5 = -0.41398$ represents the MD data within the simulation statistical accuracy over the *entire* thermodynamically stable fluid range (i.e., up to the freezing density $\rho_f = 0.9392$). The equation of state mKLM from ref. 16 was taken in calculating λ_E from

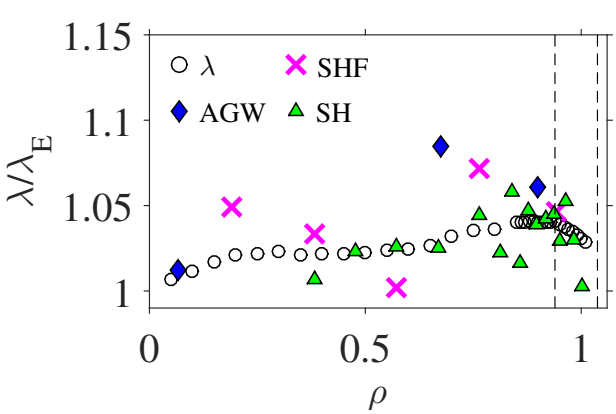

Fig. 4 Figure shows the density dependence of the ratio λ/λ_E of the hard sphere fluid. The symbols as in Fig. 3.

Table 1 The thermal conductivity and its three components (in units of $k_B\sigma^{-2}(k_BT/m)^{1/2}$) of HS fluid obtained as the limiting value of the MD data (calculated from Eqs. (4) and (5)) with $N^{-2/3}$ scaling.

ρ	λ	λ^{kk}	λ^{kc}	λ^{cc}
0.05	0.7303(4)	0.6383(4)	0.08500(7)	0.007157(4)
0.10	0.7974(9)	0.6015(7)	0.1692(2)	0.02668(3)
0.15	0.884(1)	0.5671(8)	0.2537(3)	0.06312(8)
0.20	0.993(2)	0.5339(9)	0.3387(7)	0.1202(1)
0.25	1.126(2)	0.5006(6)	0.4232(9)	0.2023(4)
0.30	1.293(2)	0.4680(8)	0.509(1)	0.3152(6)
0.35	1.493(2)	0.4335(9)	0.593(1)	0.4662(5)
0.40	1.746(4)	0.4019(6)	0.680(2)	0.664(1)
0.45	2.055(4)	0.3692(7)	0.766(2)	0.920(1)
0.50	2.437(5)	0.3401(7)	0.853(2)	1.244(2)
0.55	2.911(6)	0.3087(6)	0.942(2)	1.660(3)
0.60	3.490(6)	0.2792(5)	1.028(2)	2.183(4)
0.65	4.211(6)	0.2513(4)	1.119(2)	2.841(4)
0.70	5.119(7)	0.2253(4)	1.206(2)	3.688(5)
0.75	6.24(1)	0.2005(3)	1.295(3)	4.744(7)
0.80	7.62(1)	0.1765(3)	1.382(2)	6.061(8)
0.85	9.38(1)	0.1552(2)	1.469(3)	7.753(9)
0.86	9.78(1)	0.1511(2)	1.489(3)	8.137(9)
0.87	10.19(1)	0.1469(2)	1.505(2)	8.536(8)
0.88	10.63(1)	0.1430(2)	1.525(2)	8.966(9)
0.89	11.09(1)	0.1388(2)	1.541(2)	9.41(1)
0.90	11.56(2)	0.1349(1)	1.557(2)	9.87(1)
0.91	12.06(1)	0.1312(2)	1.576(2)	10.35(1)
0.92	12.59(1)	0.1271(1)	1.594(2)	10.87(1)
0.93	13.14(1)	0.1237(1)	1.617(2)	11.40(1)
		- metastable fluid below -		
0.94	13.73(1)	0.1204(1)	1.637(2)	11.97(1)
0.95	14.31(1)	0.1165(1)	1.652(2)	12.54(1)
0.96	14.94(2)	0.1133(2)	1.672(2)	13.15(2)
0.97	15.59(2)	0.1096(2)	1.691(2)	13.78(1)
0.98	16.28(2)	0.1064(1)	1.709(2)	14.47(2)
0.99	17.00(2)	0.1030(2)	1.728(3)	15.17(2)
1.00	17.76(2)	0.0997(1)	1.748(3)	15.91(2)
1.01	18.56(2)	0.0963(2)	1.765(3)	16.70(2)

Eq. (2). The formula in Eq. (7) for the total thermal conductivity is shown in Fig. 3 as the solid line, and Fig. 4 shows $f = \lambda/\lambda_E$. Figure 5 shows the difference between the MD generated thermal conductivity components and totals, and their Enskog predictions. The kk term dominates at low densities of ca. $\rho < 0.25$, and is essentially the total value. The difference between the MD and Enskog kk values is quite significant even at these low but finite densities. It may be seen in Fig. 5 that up to $\rho < 0.25$ the total excess thermal conductivity, $\Delta_E = \lambda - \lambda_E$ is mainly kinetic in origin (i.e., $\Delta_E \cong \Delta^{kk}$). In the dense fluid region this difference is strongly dominated by the cc-part, so $\Delta_E \approx \Delta^{cc}$. A noteworthy feature in Fig. 5 is that the cc component of Δ starts to *decrease* just above the freezing density in the direction of higher densities. Thus, up to the freezing density, ρ_f, the MD-derived, λ values progressively becomes larger than the Enskog value, λ_E with increasing density. This effect, which is observed for all the transport coefficients, may be attributed to the greater importance of successive correlated collisions with increasing density. A qualitatively different trend emerges above the freezing density. For densities, $\rho > \rho_f$, the difference for the cc component stops increasing at ρ_f and going into the metastable fluid region (see the inset in Fig. 5). The difference in the total λ behaves similarly. The trend is hardly visible in the kk and ck parts so its origin in the thermal conductivity Δ_E comes almost entirely from the cc part. Also, the λ versus density data in Fig. 3 are smoothly vary-

This journal is © The Royal Society of Chemistry [year]

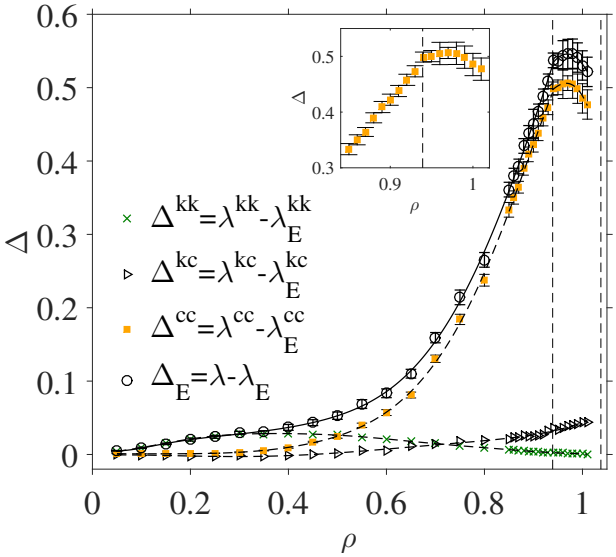

Fig. 5 The 'excess' thermal conductivity of the HS fluid in the equlibrium and metastable regions. The difference $\Delta_E = \lambda - \lambda_E$ between the components described in the legend of the thermal conductivity (Table 1) and the Enskog formula are shown. The solid and dashed lines are only to guide the eye. The vertical thin dashed lines indicate the freezing and melting densities. In the inset the density dependence of the difference, Δ^{cc}, is shown.

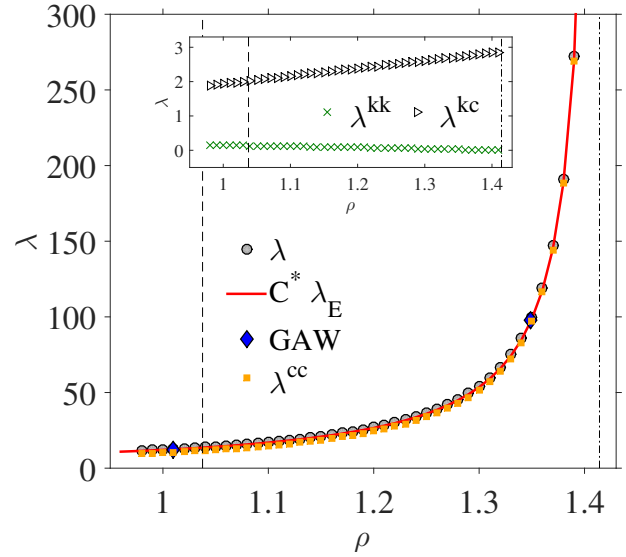

Fig. 6 Thermal conductivity and its components (kk, kc, and cc) of the hard sphere solid. The grey solid circles are the results of this work (see Table 2). The components kk, kc, cc of the thermal conductivity are also shown as green crosses, open right-triangles and orange solid squares, described on the legend. The blue solid diamonds ('GAW') represent the values from Gass *et al.*[28] extrapolated to the thermodynamic limit with the scaling formula given in Eq. (6). The red solid line represents the Enskog-like formula in Eq. (8). The vertical thin dashed line indicates the melting density ($\rho = 1.0376$ from ref. 16) and the dot-dashed line is the close packing density.

ing and can be well-represented by an equation of the form in Eq. (7), and shows no obvious signature of the freezing transition. There are at least two possible reasons why this decrease in Δ^{cc} in the metastable fluid region has not been observed until now. First, the available MD λ data were not sufficiently precise over the requisite density range to reach this conclusion. Secondly, there is no indication that D and η_s, and the equation of state $\mathscr{Z}$ behave in this way, and there would have been no motivation to have looked for it in the thermal conductivity. Figure 5 shows that the thermal conductivity is correlated with the freezing transition. From the foundations of the Enskog theory we may speculate why $\lambda^{cc} - \lambda_E^{cc}$ changes near to ρ_f. It could mean, for example, that at the freezing density many-body processes start to decrease in importance because the system starts to behave in a more solid-like manner as the particles become more rigidly confined for long times by their surrounding HS in the metastable state (which is more compatible with the 'short-time' Enskog theory).

4 Hard sphere solid

The thermal conductivity MD data of the HS crystal were extrapolated to the thermodynamic limit using Eq. (6), and the resulting values are collected in Table 2 and shown in Figure 6.

As may be seen in Fig. 6, the thermal conductivity monotonically increases with density and tends to infinity in the close packed limit (i.e., $\rho_{cp} = \sqrt{2}$), which means that very large values of λ can be achieved in the perfect HS crystal. Over the entire solid phase the dominant contribution comes from the cc component. The inset shows that the kinetic term (kk) decreases with density and its contribution is negligible, perhaps apart from in the melting region. Thus, the behaviour of λ in the solid phase can be viewed to be a continuation of the trends observed in the dense fluid phase (see Fig. 3).

Gass, Alder and Wainwright in their MD paper[28] provided evidence that the thermal conductivity of the HS solid is given to a good approximation by the Enskog formula in Eq. (2). Consistent with this rather surprising result, we have found that the following expression gives a very accurate representation of the thermal conductivity of the metastable HS solid below the melting density ($\rho_m = 1.0376$) region to nearly close packing

$$\lambda(0.98 < \rho < \rho_{cp}) = C^* \lambda_E, \tag{8}$$

where $C^* = 1.0367$ is the only fitting parameter. In the calculations of λ_E in Eq. (2) the most accurate equation of state of the HS solid to date (i.e., Eq. (7) in ref. 16),

$$\mathscr{Z} = \frac{3}{1-w} + \frac{1}{c_1 w + c_2} + A e^{B(1-w)} + C e^{D(1-w)} + E, \tag{9}$$

was used, where $w = \rho/\rho_{cp}$, $c_1 = 1$ $c_2 = 3/2$, and $A = 0.025882$, $B = 8.689$, $C = 3.5433 \cdot 10^{-6}$, $D = 34.377$, $E = -1.85973$. The ratio λ/λ_E is shown in Fig. 7, in which it is observed that the one-parameter formula of Eq. (8) describes well the entire solid region. The constant C^* is close to but not equal to unity, and the small difference from unity is crucial in obtaining agreement with the MD data. With Eqs. (2) and (9) the limiting regions near melting and close packing can be analysed.

4.1 The $\rho \to \rho_{cp}$ limit

For the dense HS solid the first and second terms in Eq. (2) become negligible compared to the third term. Consequently in this

Table 2 The thermal conductivity and its three components (in units of $k_B\sigma^{-2}(k_BT/m)^{1/2}$) of the HS solid obtained as the large system limiting value of the MD data (calculated from Eqs. (4) and (5)) with $N^{-2/3}$ scaling.

ρ	λ	λ^{kk}	λ^{kc}	λ^{cc}
0.98	11.58(3)	0.1447(5)	1.878(6)	9.56(3)
0.99	11.88(6)	0.1435(7)	1.909(9)	9.83(5)
1.00	12.19(6)	0.1408(6)	1.925(9)	10.12(5)
1.01	12.58(4)	0.1392(5)	1.955(8)	10.48(3)
1.02	12.95(6)	0.1365(6)	1.973(9)	10.84(5)
1.03	13.39(6)	0.1344(6)	2.004(9)	11.25(5)
		- metastable solid above -		
1.04	13.81(5)	0.1315(4)	2.022(7)	11.65(5)
1.05	14.24(6)	0.1286(4)	2.039(8)	12.08(6)
1.06	14.78(4)	0.1263(5)	2.069(7)	12.58(4)
1.07	15.30(6)	0.1233(6)	2.090(9)	13.09(5)
1.08	15.84(4)	0.1204(3)	2.108(6)	13.61(4)
1.09	16.44(7)	0.1176(4)	2.134(9)	14.19(6)
1.10	17.07(5)	0.1143(3)	2.151(7)	14.81(5)
1.11	17.79(8)	0.1116(5)	2.181(9)	15.50(7)
1.12	18.50(8)	0.1085(4)	2.202(9)	16.19(7)
1.13	19.31(8)	0.1055(6)	2.228(9)	16.98(7)
1.14	20.18(9)	0.1023(5)	2.251(9)	17.83(8)
1.15	21.05(7)	0.0992(3)	2.271(7)	18.68(7)
1.16	22.06(6)	0.0957(3)	2.292(8)	19.67(6)
1.17	23.18(8)	0.0925(3)	2.322(8)	20.77(7)
1.18	24.30(9)	0.0891(4)	2.338(9)	21.87(9)
1.19	25.57(9)	0.0857(3)	2.361(8)	23.12(8)
1.20	27.0(1)	0.0824(4)	2.38(1)	24.5(1)
1.21	28.4(1)	0.0786(3)	2.40(1)	25.9(1)
1.22	30.1(1)	0.0753(3)	2.43(1)	27.6(1)
1.23	31.9(1)	0.0716(3)	2.44(1)	29.4(1)
1.24	34.2(1)	0.0682(2)	2.48(1)	31.6(1)
1.25	36.5(1)	0.0645(3)	2.50(1)	33.9(1)
1.26	39.0(1)	0.0606(2)	2.51(1)	36.4(1)
1.27	42.1(1)	0.0570(2)	2.54(1)	39.5(1)
1.28	45.6(2)	0.0534(2)	2.57(1)	42.9(2)
1.29	49.5(2)	0.0494(2)	2.58(1)	46.9(2)
1.30	54.2(2)	0.0457(2)	2.61(1)	51.5(2)
1.31	59.9(2)	0.0419(1)	2.63(1)	57.2(2)
1.32	66.7(2)	0.0379(2)	2.65(1)	64.0(2)
1.33	75.1(2)	0.0340(1)	2.67(1)	72.4(2)
1.34	85.7(3)	0.0301(1)	2.69(1)	83.0(3)
1.35	99.8(4)	0.02611(5)	2.71(1)	97.0(4)
1.36	119.1(3)	0.02214(8)	2.74(1)	116.3(3)
1.37	146.9(4)	0.01814(5)	2.76(1)	144.1(4)
1.38	191.2(7)	0.01408(5)	2.78(1)	188.4(7)
1.39	272(1)	0.01000(4)	2.81(1)	269.3(9)
1.40	466(2)	0.00590(3)	2.83(1)	463(2)
1.41	1547(7)	0.001756(6)	2.84(1)	1582(7)

region the thermal conductivity becomes a simple function of $\mathscr{Z}$,

$$\lambda \cong C^*\lambda_0\rho b_2 \cdot 0.7574\mathscr{Z} = const \cdot \rho\mathscr{Z}. \tag{10}$$

In the high density limit near to close-packing the first term is much larger than the other four in the formula for $\mathscr{Z}$ in Eq. (9), which leads to the accurate simplification,

$$\mathscr{Z}(\rho \to \rho_{cp}) = \frac{3}{1-w}. \tag{11}$$

With this formula for $\mathscr{Z}$ the limiting formula for the thermal conductivity of the HS crystal is,

$$\lambda(\rho \to \rho_{cp}) = \Omega\left[\frac{\rho}{\rho_{cp}-\rho}\right], \tag{12}$$

where the constant, $\Omega = C^*\lambda_0 b_2 \cdot 0.7574 \cdot 3\rho_{cp} = 4.7289$. The predicted limiting behaviour given in Eq. (12) is consistent with

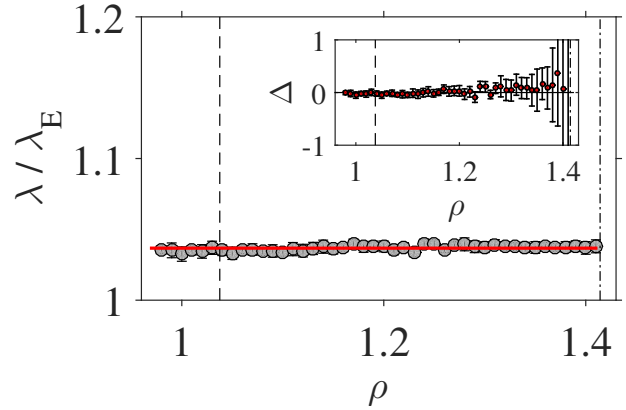

Fig. 7 The density dependence of the ratio, λ/λ_E, of the hard sphere solid. The grey solid circles are the results of this work (see Table 2) and the red solid line represents the value of C^* from the Enskog-like formula in Eq. (8). In the inset the difference, $\Delta = \lambda - C^*\lambda_E$, is shown. The vertical lines have the same significance as those in Fig. 6.

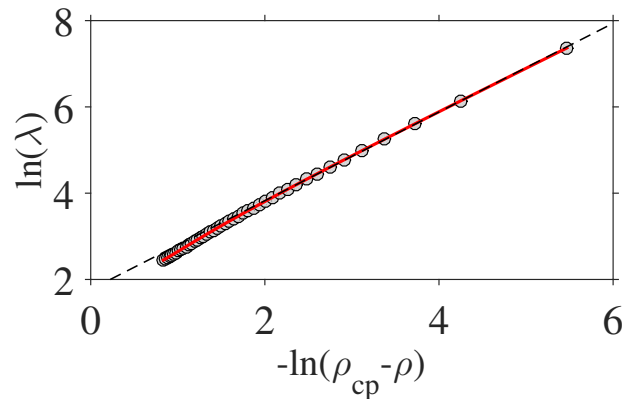

Fig. 8 The quantity, $\ln(\lambda)$, as a function of $-\ln(\rho_{cp}-\rho)$ in the high density limit ($\rho \to \rho_{cp}$). The density increase (from left to right) from 0.98 up to close packing. The grey solid circles are the results of this work (taken from Table 2). The red solid line is the expression for the thermal conductivity given in Eq. (8) and the dashed line represents the linear convergence of the data found in the high density limit (see Eq. (12)) extended to lower densities.

the plot in Fig. 8. This divergence and singularity in the thermal conductivity is probably a unique feature of hard spheres, as such sharp divergences are not typically observed for experimental molecular systems. For example, the Vogel-Fulcher-Tammann (VFT) equation describing the temperature dependence of the dielectric spectrum relaxation time of viscous liquids (which has a singularity) is another example where no convincing evidence for a singularity is seen in experimentally systems.[29] There may be analogous features in highly agitated granular systems though, where the particles are better represented by the HS potential.

4.2 The $\rho \approx \rho_m$ region

For densities near the melting transition the contributions from the first and second terms in Eq. (2) are small, but in contrast to the close-packed limit, they are not negligible. In this density region the first term in Eq. (9) is still the main contribution to $\mathscr{Z}$. Thus, near melting, the solid phase HS thermal conductivity

This journal is © The Royal Society of Chemistry [year]

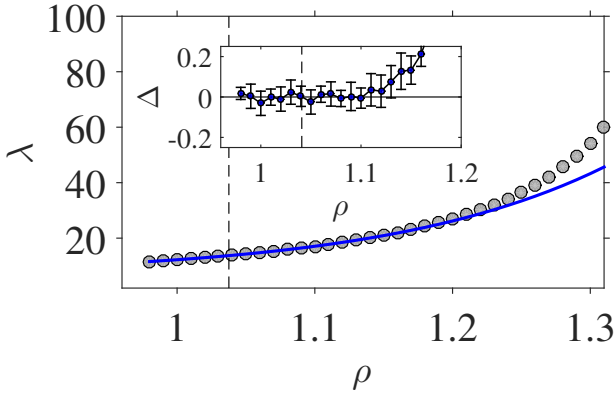

Fig. 9 The thermal conductivity λ as a function of density near the transition region ($\rho \approx \rho_m$). The grey solid circles are the results of this work (Table 2). The blue solid line represents expression in Eq. (13). In the inset the difference, $\Delta = \lambda - \lambda_{exp}$, between the analytic formula and data of this work is shown.

can be represented as the sum of two parts, the leading term consisting of $3/(1-w)$ and the second containing all other terms. At $\rho \approx \rho_m$ the term $3/(1-w) \cong a(1-b(\rho_m-\rho)) \approx a\exp(-b(\rho_m-\rho))$ where the constants $a = 3\rho_{cp}/(\rho_{cp}-\rho_m)$ and $b = 1/(\rho_{cp}-\rho_m)$. Therefore, the first part can be represented by an exponential to a good approximation, while the second contribution to λ is about ten times smaller and is a nearly density independent function. Note that a and b are not fit parameters but are expressed in terms of the known quantities, ρ_m and ρ_{cp} only. Therefore near the melting density the thermal conductivity must be well represented by an exponential function and the closer the density is to ρ_m the better the approximation is. In fact the λ is very well represented by this limiting dependence at least for the density range $|\rho-\rho_m| < 0.06$.

A good exponential representation of the solid HS thermal conductivity at higher densities can be achieved also with the same general exponential form using,

$$\lambda_{exp}(\rho) \approx A' e^{B'\rho} + C' \tag{13}$$

where $A' = 0.010373$, $B' = 6.28358$ and $C' = 6.65986$ are coefficients fitted to the λ values from Table 2. Figure 9, which shows the density dependence of λ, demonstrates that the approximation in Eq. (13) reproduces the simulation λ values very well for a considerable part of the solid phase i.e., for all densities where *ca.* $\rho < 1.1$. Note the fit is also very good for the metastable solid state (i.e. for $\rho < \rho_m$). Therefore to summarise, a simple exponential formula can be used to represent the thermal conductivity of hard spheres over a significant part of the solid melting region, certainly for *ca.* $\rho < 1.1$. It has been found that the thermal conductivity depends exponentially on density for a number of solid systems,[30] and the present results show this to be the case also for the HS solid.

4.3 Enskog theory for the HS solid thermal conductivity

Some understanding of the origin of Eq. (8) can be obtained within the framework of the kinetic theory developed by Kirpatrick, Das, Ernst and Piasecki (KDEP)[31] for a HS crystal. The authors applied the revised Enskog kinetic theory (RET)[32,33] and extended the Enskog expressions for the transport coefficients of the dilute fluid state to a HS crystal. It was shown that in this case, due to crystal anisotropy, the complete Enskog thermal conductivity is more complex than for the (isotropic) liquid. In particular the derived expression, λ_{RET}, for the thermal conductivity contains a function, F', which measures the anisotropy in the HS-crystal, and vanishes in the isotropic case. As short-time processes determine the transport coefficients in the solid state and the RET is exact for short times it is reasonable to assume that λ_{RET} describes the thermal conductivity of the HS crystal[31]. The resulting RET thermal conductivity is,[31]

$$\begin{aligned}\lambda_{RET} =& \lambda_0 b_2 \rho \left[1 + \frac{6\mathscr{Z}}{5} + \left(\frac{9}{25} + \frac{32}{25\pi}\right)\mathscr{Z}^2 \right.\\ &- \left(\frac{1}{3\mathscr{Z}} + \frac{2}{5} + \left(\frac{3}{25} + \frac{32}{75\pi}\right)\mathscr{Z}\right)F' \\ &\left. + \left(\frac{8}{15\mathscr{Z}} + \frac{32}{75} - \frac{64}{75\pi}\right)F'^2\right] \times \left(\mathscr{Z} - \frac{F'}{3} - \frac{2F'^2}{3\mathscr{Z}}\right)^{-1}.\end{aligned} \tag{14}$$

Note that in ref. 31 the symbol F_1 is used for $\mathscr{Z}$ (i.e., the non-ideal gas part of the equation of state of the HS crystal). For the isotropic liquid, $F' = 0$, and the above expression reduces to the Enskog formula given in Eq. (2). Thus, assuming $\lambda \cong \lambda_{RET}$, the "constant" in Eq. (8) can be a quite complicated function of $\mathscr{Z}$ and F' which can be expressed simply as $C^*(\mathscr{Z}, F') = \lambda_{RET}/\lambda_E$ with the condition $C^*(\mathscr{Z}, F' = 0) = 1$. To obtain λ_{RET} the quantity, F', is required. A definition of F' is given in Eq. (4.4d), of ref. 31 but its calculation is not straightforward. However, if we know λ then F' can be obtained from Eq. (14) by setting λ_{RET} to λ for the purpose of this exercise. After rearrangement of Eq. (14) a simple quadratic equation for F' can be derived, which has the following solution,

$$F' = \frac{-Q_2 - \sqrt{Q_2^2 - 4Q_1Q_3}}{2Q_1}, \tag{15}$$

where $Q_1 = -2\lambda/3\mathscr{Z} - \lambda_0 b_2 \rho\,(8/15\mathscr{Z} + 32/75 - 64/75\pi)$, $Q_2 = -\lambda/3 + \lambda_0 b_2 \rho\,(1/3\mathscr{Z} + 2/5 + (3/25 + 32/75\pi)\,\mathscr{Z})$ and $Q_3 = -3\mathscr{Z}Q_2$. Equation (15) gives in effect an explicit expression for the density dependence of F'. This solution is shown in Fig. 10 (the second solution, $F' < 0$ for all densities, is not a physical one as it gives e.g., a negative viscosity in Eq. (4.6),[31]). In this way a fairly accurate representation of the F' function is obtained which is necessary in the description of the transport coefficients of the HS crystal within the RET framework. A useful result is apparent in the inset where it is seen that F' can be expressed as a simple function of $\mathscr{Z}$. Taking into account the accuracy of the compressibility factor and λ (Table 2) used in the calculations, the following relationship is evident, $F' = \xi\mathscr{Z}$, where $\xi = -0.0095\rho + 0.1709$ is a linear function of density with almost zero slope and which can be well represented by a value close to 0.16.

With this relation for F' the expression in Eq. (14) for the λ_{RET} simplifies and can be expressed by $C^*\lambda_E$, where $C^* \cong 1.0367$ is

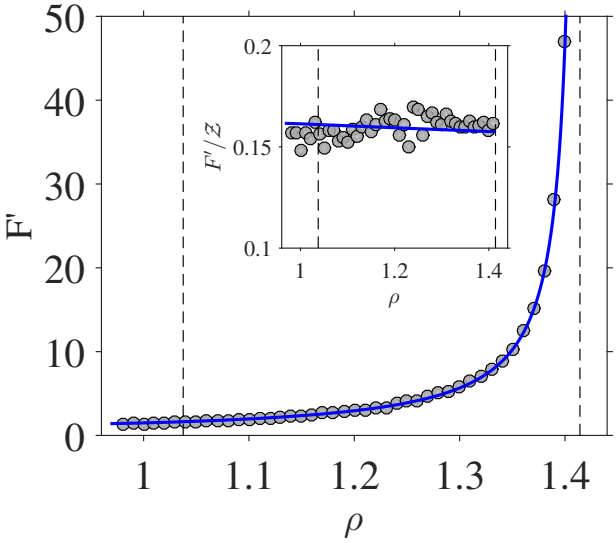

Fig. 10 The function F' in Eq. (15) obtained as the solution of Eq. (14). The grey solid circles represent the solution taking λ from Table 2 and using $\mathscr{Z} \equiv \mathscr{Z}_{MD}$ (where $\mathscr{Z}_{MD} = Z_{MD} - 1$ is the compressibility factor calculated for the same densities as λ). The blue solid line represents the solution for F' using the formulae, $\lambda \equiv C^* \lambda_E$ (in Eq. (8)) and $\mathscr{Z}$ from Eq. (9). In the inset, the ratio $F'/\mathscr{Z}$ is given, where symbols and line has the same meaning as in the main figure.

density independent or has such a weak density dependence that it can be ignored in practice.

In other words, from the fact that λ is represented by λ_{RET} the F'-function (the solution in Eq. (15)) is determined, which can be represented very well by the relation $F' = \xi \mathscr{Z}$. This in turn yields the HS solid thermal conductivity in Eq. (14) in the form $C^*(\mathscr{Z}, F')\lambda_E$ (Eq. (8)) where $C^*(\mathscr{Z}, F') \cong 1.0367$.

5 λ−dependence on other quantities

In this section the relationships between $\lambda(\rho)$ and various other properties of the HS system are discussed. For example, there is a longstanding interest in the pressure dependence of thermal conductivity e.g., in geology.[34–36] As an accurate equation of state has been established for the HS fluid and crystal, the pressure dependence of the thermal conductivity, $\lambda(P)$, and its various pressure derivatives can be obtained directly from $\lambda(\rho)$. In this way, a number of quantities involving $\lambda(\rho)$, $\lambda(P)$, $ln(\lambda(\rho))$ and $ln(\lambda(P))$, and their derivatives, can now be readily derived. Also, scaling laws which propose a relationship between λ and properties such $\mathscr{Z}$ or excess entropy can be tested. Three examples of this reparameterisation of $\lambda(\rho)$ were carried out and are discussed below.

Under compression vibrational frequencies increase and the lattice conductivity increases with pressure as a result.[36,37] The pressure dependence of the HS thermal conductivity is shown in Fig. 11a, which indicates that the HS crystal λ is practically linear with P. This simple dependence is a direct consequence of the relation in Eq. (8) and the dominant role of the $\sim \rho \mathscr{Z}$ component. For the HS crystal the thermal conductivity scales with the pressure as, $\lambda \cong 1.116P + 2.146$. Many crystals display a near-linear dependence of λ on pressure.[34,38,39] From our

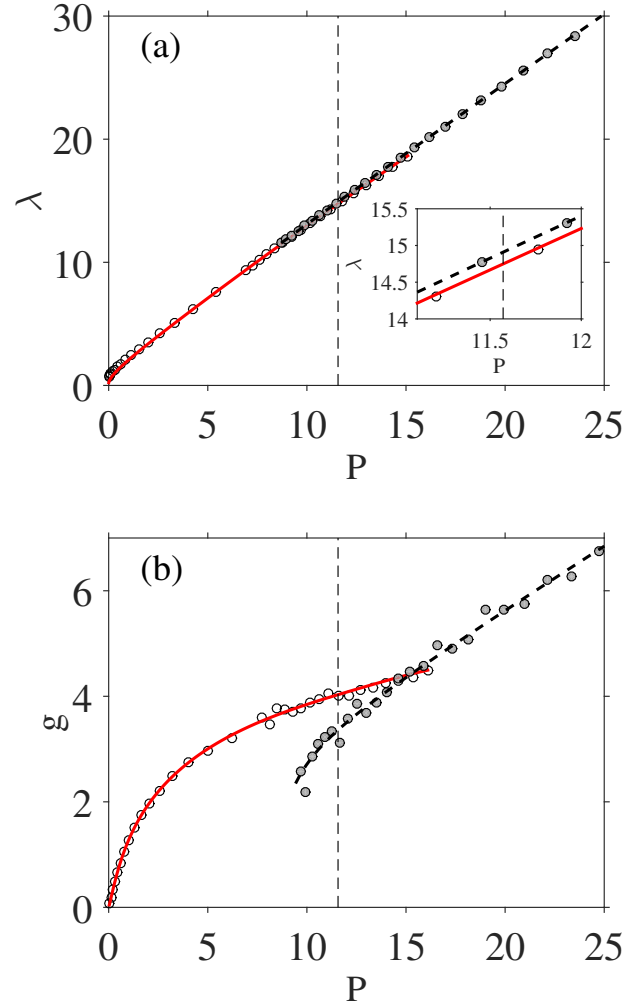

Fig. 11 In frame (a) the pressure dependence of the thermal conductivity, λ, is shown, and in frame (b) the derivative, $g = (\partial \ln\lambda / \partial \ln\rho)_T$ as a function of pressure P is given. In both subplots the open and grey solid circles are the results of this work for fluid λ (data given in Table 1) and the solid phase λ (from Table 2), respectively. The solid red line represents the expression for the fluid phase thermal conductivity given in Eq. (7). The black dashed line is the formula for the solid phase thermal conductivity taken from Eq. (8). The vertical dashed line indicates the coexistence pressure, $P_{co} = 11.5712$.[16]

HS results such a dependence follows directly from the relation $C^* \lambda_E$. The HS thermal conductivity is almost linear in P in the fluid as well, particularly in the dense equilibrium and metastable regions.

The divergence of the thermal conductivity in the close-packed limit follows naturally from the accompanying divergence of the pressure. The speed of sound approaches infinity at this point and the stress and energy are 'immediately' transferred across the domain. It is reasonable to assume that this general feature of a rapidly increasing thermal conductivity with pressure in the high density solid is not unique to hard spheres but also applies to other systems in which the particles interact with sufficiently steeply repulsive hard potentials. The effect of a change of λ across a transition under pressure is also of a practical interest. It has been found experimentally that the

This journal is © The Royal Society of Chemistry [year]

change, $\Delta\lambda$, is discontinuous across the first-order transition and for many crystals is positive but it can be negative.[34,40] As seen in the inset in Fig. 11a, in the case of the HS system, the difference across the melting-freezing transition is positive but relatively small in magnitude.

A useful parameter which characterises the volume or pressure dependence of λ of various materials is $g = (\partial ln\lambda/\partial ln\rho)_T$[30,41] (which has been also referred to as the 'Bridgman parameter'). It has been observed that for liquids g is usually about 3 and typical values for crystals are in the range, $6-10$. Figure 11b shows the dependence of the g-parameter as a function of pressure, which shows that for the hard sphere system g increases with pressure (and therefore density) and, apart from at very high pressures (densities), is quantitatively in the same numerical range as found for more complex molecular systems.

A third example of another property-dependence is in terms of the excess (or residual) entropy or S_{ex}, which has been studied extensively since the pioneering work of Rosenfeld.[42–45] For the fluid phase the excess entropy was calculated from, $S_{ex} = -\int_0^{\rho'} d\rho' \mathscr{Z}(\rho')/\rho'$, where $\mathscr{Z}$ is the mKLM equation of state of the HS fluid taken from ref. 16. For the solid phase the excess entropy was calculated from $S_{ex} = -(F(\rho_{ref}) - F(\rho)_{ideal}) - \int_0^{\rho'} d\rho' Z(\rho')/\rho'$, where $\rho_{ref} = 1.04086$ is the reference state number density, and $F(\rho_{ref}) = 4.9590$ is the Helmholtz free energy at that density. The $F(\rho)_{ideal}$ is the Helmholtz free energy for the ideal gas, and Z is the Z_{S2} equation of state of HS solid from ref. 16 (or Eq. (9) where $Z = \mathscr{Z} + 1$). Note that the excess entropy is negative.

Our analysis of the HS $\lambda(S_{ex})$ behaviour leads to the following conclusions. A simple formula for $\lambda(S_{ex})$ for the HS fluid across the whole density range was not found. This conclusion was also reached for the thermal conductivity of real molecular systems in refs. 46,47 and the model Lennard-Jones fluid in ref. 48. The dimensionless thermal conductivity does not show a single-variable dependence in terms of the excess entropy. However local S_{ex}-scaling of thermal conductivity is observed for the HS fluid. For a limited range of fluid densities it is possible to propose a reasonably accurate analytic form for $\lambda(S_{ex})$. In fact, such local scaling laws are often formulated e.g., Rosenfeld's exponential scaling (i.e., $\lambda \propto \exp(-S_{ex}^p)$,[49] where p is a positive constant) is usually only obeyed for a limited density range, and not for the entire fluid phase. In the inset of Fig. 12 it is shown that there is a straight line on a ln-ln scale which represents well most of the points. This indicates that the simple relation, $\lambda = \lambda_0 + A_f(-S_{ex})^{B_f}$, where $A_f = -0.2723$ and $B_f = 1.8030$, is obeyed to a good approximation. However, this simple scaling does not hold at low densities ($\rho < 0.6$) but, as is visible in the main figure, on a lin-lin scale it correlates λ and S_{ex} very well for most fluid phase (including the metastable region). It may be speculated that the quality of this scaling increases as the cc component of the collision sequence becomes more dominant. The value of B_f may have a statistical mechanical significance.

For the crystal phase $\lambda(S_{ex})$ is shown in the bottom right inset of Fig. 12, where on a ln-lin scale it is almost a straight line, which signifies the simple type of scaling, $\lambda = A_s + B_s \exp(-C_s S_{ex})$, where $A_s = -1.299$, $B_s = 2.073$, and $C_s = 0.334$. Importantly therefore,

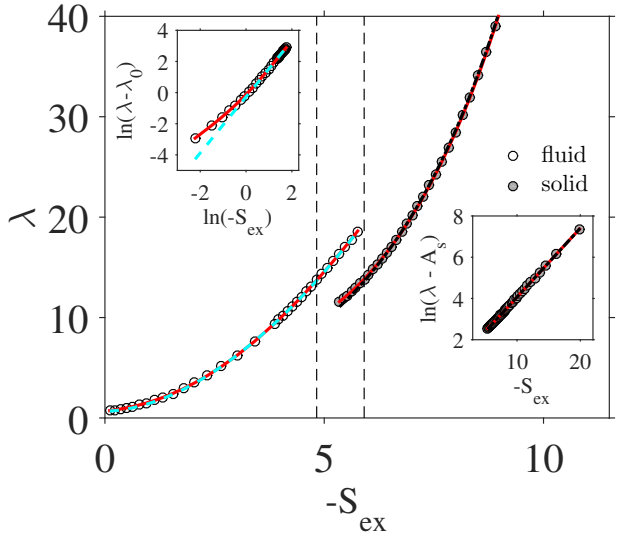

Fig. 12 The thermal conductivity, λ, as a function of excess entropy $-S_{ex}$ for the fluid and solid phases. The open and grey solid circles are the results of this work for the fluid (see Table 1) and for the solid (see Table 2), respectively. The solid red lines are generated from thermal conductivity expressions for fluid and solid phases, in Eqs. (7) and (8), respectively. The cyan dashed line is the empirical scaling formula for the fluid phase, $\lambda = \lambda_0 + A_f(-S_{ex})^{B_f}$. This curve is also presented in the top left inset in the logarithmic form, $\ln(\lambda - \lambda_0)$ *vs.* $\ln(-S_{ex})$. The black dot-dashed line shown on the right is the corresponding scaling formula for the solid, as $\lambda = A_s + B_s \exp(-C_s S_{ex})$. This curve is also presented in right bottom inset in the form, $\ln(\lambda - A_s)$ *vs.* $-S_{ex}$. The appropriate coefficients for these formulae are given in the main text. The two vertical dashed lines from left to right denote the freezing and melting boundaries, respectively.

apart from small deviations in the metastable region (below the melting density), this formula represents quite accurately the thermal conductivity of the whole crystalline phase. Therefore, for the HS crystal the thermal conductivity scales well with the excess entropy. Also it has basically the same analytic form as that proposed by Rosenfeld for fluids.[42,43]

6 Conclusions

This work reports a new set of hard sphere (HS) thermal conductivity coefficient, λ, data obtained by Molecular Dynamics (MD) computer simulation, over a density range covering the dilute fluid to near the close-packed solid. This includes the freezing-melting transition region. The study constitutes the most comprehensive and accurate representation of the thermal conductivity of the HS system to date, using a very large number, N, of particles and long simulations by traditional standards.

The total λ and its three collision sequence components are given for the fluid, solid and metastable fluid regions. These are fitted to separate analytic formulae for the fluid and crystal branches.

The $N-$dependence of the thermal conductivity is shown to follow well a $N^{-2/3}$ analytic form over a wide range of system sizes. For the fluid, the density dependence of, λ, can be expressed as the product of the Enskog formula, λ_E and a density-dependent term, f which has been formulated as a polynomial expansion fit to the MD data. The differences between Enskog and simulation

values in the fluid state increase progressively with density but starts to decrease near the freezing density in the metastable region.

Alder *et al.* in 1970,[28] discovered by MD simulations that the thermal conductivity of the solid is predicted quite well by Enskog theory. We have confirmed this conclusion and have shown, further, that the formula, $\lambda = C^* \lambda_E$, where C^* is very close to unity, fits the MD data well over the entire solid region (including the solid metastable region). The origin of C^* is discussed using the revised Enskog theory (RET) for the HS crystal.

The relatively good agreement between the MD and Enskog predictions for the thermal conductivity of the HS fluid phase, when compared to the self-diffusion coefficient and shear viscosity (see ref. 16 for their behaviour) is consistent with previous studies of the collective modes of the HS fluid [50–52] (some more recent discussion on analysing collective excitations in fluids is presented in refs. 53,54). Also the extended heat mode is quite insensitive to the details of the interaction potential suitable for normal small molecules (in contrast to the longitudinal sound mode).[55] Therefore their properties can be understood quite well within the framework of Enskog theory.[52] The thermal diffusivity of the HS system has a minimum at a density of *ca.* 0.35 in agreement with the behaviour of the inverse power fluid with an exponent of 12.[56]

Alder *et al.* argued that as Enskog theory (ET) is based on representing the short-time decay processes, these must dominate the thermal conductivity of hard sphere solids. In fluids, in contrast, many-body interactions have been shown to set up velocity fields which persist for many mean collision times. In hard sphere solid systems, long-time correlations and collective processes between the molecules are suppressed by the confinement of each particle by its nearest neighbours, hence the success of ET for the hard sphere thermal conductivity of the solid. The significance of this rather surprising result is that there is an explicit relationship between a transport coefficient and the equation of state for the entire solid phase. The consequence of this, which we have shown in the MD data, is that the thermal conductivity diverges in the close-packed solid limit. This divergence has the algebraic form, $\Omega\rho/(\rho_{cp} - \rho)$, where Ω is a constant expressible in terms of known basic quantities, ρ is the number density, and ρ_{cp} is the close-packed solid density. The physical significance of Ω which may take into account the crystal structure is not well understood. In the low density fluid limit the thermal conductivity is proportional to density where the equivalent quantity to Ω is $\lambda_0 b_2$.

In Honda's treatment of the hard sphere FCC crystal[57] it was shown that at high density the effective HS particle interaction can be considered to be harmonic, which leads to an effective harmonic Hamiltonian. By using the dispersion relations of the lattice vibrations, the phonon branches were investigated. It is known that the phonon-based thermal conductivity diverges for a 3D harmonic solid because there is no dissipation mechanism. Therefore it follows that the increase and divergence of the HS thermal conductivity in the ideal HS crystal is probably because, on increasing density, the solid exhibits behaviour which can approximately be described by a harmonic solid. This leads to the somewhat paradoxical conclusion, that for a system with an extremely anharmonic interaction, harmonic behaviour can emerge near close packing, and thereby give rise to a divergence of the thermal conductivity. There is therefore a 'symmetry' in the thermal conductivity behaviour, in that Enskog theory gives the low density limit accurately and also the high dense solid-state limit to a good approximation. The first limit is determined only by the purely kinetic (kk) part of the collision sequence, and the second limit is determined only by the purely interaction part (cc).

The HS crystal thermal conductivity can therefore be arbitrarily large, which could be exploited in some practical applications of appropriate hard particle systems. The HS shear viscosity of the metastable fluid diverges at about the glass transition density which is much lower than ρ_{cp},[16] but the shear viscosity may also still show a similar divergence to the thermal conductivity in the close-packed solid limit.

For the HS solid and dense fluid it was found that the thermal conductivity is nearly linear in pressure, as has been observed experimentally for a number of solids. Another interpretation of the divergence of the thermal conductivity in the close-packed limit is that we know the thermal conductivity is proportional to the pressure in the solid region, which diverges in the close-packed limit. As a consequence, in this limit the collision rate will tend to infinity and the mean time between collisions goes to zero. As a result it may not be too surprising therefore that the thermal resistance is zero in the close-packed solid limit.

The thermal conductivity does not show a simple excess entropy scaling over the whole fluid phase, but Rosenfeld's exponential relationship can be fitted to the simulation data for the solid to a very good degree of accuracy.

It has been demonstrated here that the density and pressure dependence of the thermal conductivity of the hard sphere fluid and solid shares a number of generic trends with those of some chemical systems with quite different force fields and molecular architectures. This is despite the fact that traditional theoretical formulation of solid thermal conductivity is in terms of phonons, whereas the HS solid can be represented by an Enskog theory which is based on random collisions and not phonons. The thermal conductivity of liquids and solids is an important property in many technological applications, for example in solid and liquid-based cooling devices. The trends discovered in this work could be used in improving design criteria for these systems.

Conflicts of interest

There are no conflicts to declare.

Acknowledgements

Some of the MD calculations were performed at the Poznań Supercomputing and Networking Center (PCSS). DMH would like to thank Dr. T. Crane (Department of Physics, Royal Holloway, University of London, UK) for helpful software support.

This journal is © The Royal Society of Chemistry [year]

References

1 H. C. Longuet-Higgins and J. A. Pople, *The Journal of Chemical Physics*, 1956, **25**, 884–889.

2 S. A. Rice, J. G. Kirkwood, J. Ross and R. W. Zwanzig, *The Journal of Chemical Physics*, 1959, **31**, 575–583.

3 B. J. Alder, D. M. Gass and T. E. Wainwright, *The Journal of Chemical Physics*, 1970, **53**, 3813–3826.

4 H. Sigurgeirsson and D. M. Heyes, *Molecular Physics*, 2003, **101**, 469–482.

5 L. Lue, *The Journal of Chemical Physics*, 2005, **122**, 044513.

6 M. J. Assael, N. K. Dalaouti, J. H. Dymond and E. P. Feleki, *International Journal of Thermophysics*, 2000, **21**, 367–375.

7 N. Xu, V. Vitelli, M. Wyart, A. J. Liu and S. R. Nagel, *Physical Review Letters*, 2009, **102**, 038001.

8 O. Kravchenko and M. Thachuk, *The Journal of Chemical Physics*, 2012, **136**, 044520.

9 D. H. Kumar, H. E. Patel, V. R. R. Kumar, T. Sundararajan, T. Pradeep and S. K. Das, *Physical Review Letters*, 2004, **93**, 144301.

10 J. Eapen, J. Li and S. Yip, *Physical Review Letters*, 2007, **98**, 028302.

11 J. Armstrong and F. Bresme, *Physical Chemistry Chemical Physics*, 2014, **16**, 12307.

12 C. Moir, L. Lue, J. D. Gale, P. Raiteri and M. N. Bannerman, *Physical Review E*, 2019, **99**, 030102(R).

13 J. J. Erpenbeck, *Physical Review A*, 1989, **39**, 4718–4731.

14 J. J. Erpenbeck, *Physical Review A*, 1992, **45**, 2298–2307.

15 M. N. Bannerman and L. Lue, *The Journal of Chemical Physics*, 2009, **130**, 164507.

16 S. Pieprzyk, M. N. Bannerman, A. C. Brańka, M. Chudak and D. M. Heyes, *Physical Chemistry Chemical Physics*, 2019, **21**, 6886–6899.

17 T. G. C. Sydney Chapman, *The Mathematical Theory of Non-Uniform Gases*, Cambridge University Press, 1991.

18 J. J. Erpenbeck and W. W. Wood, *Physical Review A*, 1991, **43**, 4254–4261.

19 D. M. Heyes, *The Liquid State*, Wiley-Blackwell, 1997.

20 S. Loyalka, E. Tipton and R. Tompson, *Physica A: Statistical Mechanics and its Applications*, 2007, **379**, 417–435.

21 J. J. Erpenbeck, *Physical Review E*, 1995, **51**, 4296–4308.

22 E. Helfand, *Physical Review*, 1960, **119**, 1–9.

23 S. Viscardy and P. Gaspard, *Physical Review E*, 2003, **68**, 041204.

24 K.-S. Kim, M. H. Han, C. Kim, Z. Li, G. E. Karniadakis and E. K. Lee, *The Journal of Chemical Physics*, 2018, **149**, 044510.

25 M. N. Bannerman, R. Sargant and L. Lue, *J. Comput. Chem.*, 2011, **32**, 3329–3338.

26 M. P. Allen and D. J. Tildesley, *Computer Simulation of Liquids*, Oxford University Press, Oxford, 2017.

27 S. W. Smith, C. K. Hall and B. D. Freeman, *The Journal of Chemical Physics*, 1995, **102**, 1057–1073.

28 D. Gass, B. Alder and T. Wainwright, *Journal of Physics and Chemistry of Solids*, 1971, **32**, 1797–1800.

29 T. Hecksher, A. I. Nielsen, N. B. Olsen and J. C. Dyre, *Nature Physics*, 2008, **4**, 737–741.

30 S. Stackhouse, L. Stixrude and B. B. Karki, *Physical Review Letters*, 2010, **104**, 208501.

31 T. R. Kirkpatrick, S. P. Das, M. H. Ernst and J. Piasecki, *The Journal of Chemical Physics*, 1990, **92**, 3768–3780.

32 H. van Beijeren and M. H. Ernst, *Journal of Statistical Physics*, 1979, **21**, 125–167.

33 A. Santos, J. Montanero, J. Dufty and J. Brey, *Physical Review E*, 1998, **57**, 1644–1660.

34 R. G. Ross, P. Andersson, B. Sundqvist and G. Backstrom, *Reports on Progress in Physics*, 1984, **47**, 1347–1402.

35 K. V. Tretiakov and S. Scandolo, *The Journal of Chemical Physics*, 2004, **120**, 3765–3769.

36 N. de Koker, *Earth and Planetary Science Letters*, 2010, **292**, 392–398.

37 W.-P. Hsieh, B. Chen, J. Li, P. Keblinski and D. G. Cahill, *Physical Review B*, 2009, **80**, 180302(R).

38 K. V. Tretiakov and S. Scandolo, *The Journal of Chemical Physics*, 2004, **121**, 11177.

39 A. M. Hofmeister, *Proceedings of the National Academy of Sciences*, 2007, **104**, 9192–9197.

40 G. A. Slack and R. G. Ross, *Journal of Physics C: Solid State Physics*, 1985, **18**, 3957–3980.

41 B. Hakansson and R. G. Ross, *International Journal of Thermophysics*, 1985, **6**, 353–365.

42 Y. Rosenfeld, *Physical Review A*, 1977, **15**, 2545–2549.

43 Y. Rosenfeld, *Journal of Physics: Condensed Matter*, 1999, **11**, 5415–5427.

44 J.-M. Bomont and J.-L. Bretonnet, *Chemical Physics*, 2014, **439**, 85–94.

45 S. Pieprzyk, D. M. Heyes and A. C. Brańka, *Physical Review E*, 2014, **90**, 012106.

46 M. Hopp and J. Gross, *Industrial & Engineering Chemistry Research*, 2017, **56**, 4527–4538.

47 M. Hopp, J. Mele, R. Hellmann and J. Gross, *Industrial & Engineering Chemistry Research*, 2019, **58**, 18432–18438.

48 I. H. Bell, R. Messerly, M. Thol, L. Costigliola and J. C. Dyre, *The Journal of Physical Chemistry B*, 2019, **123**, 6345–6363.

49 J. C. Dyre, *The Journal of Chemical Physics*, 2018, **149**, 210901.

50 W. E. Alley and B. J. Alder, *Physical Review A*, 1983, **27**, 3158–3173.

51 W. E. Alley, B. J. Alder and S. Yip, *Physical Review A*, 1983, **27**, 3174–3186.

52 C. Bruin, J. Michels, J. V. Rijs, L. D. Graaf and I. D. Schepper, *Physics Letters A*, 1985, **110**, 40–43.

53 N. P. Kryuchkov, V. V. Brazhkin and S. O. Yurchenko, *The Journal of Physical Chemistry Letters*, 2019, **10**, 4470–4475.

54 N. P. Kryuchkov, L. A. Mistryukova, V. V. Brazhkin and S. O. Yurchenko, *Scientific Reports*, 2019, **9**, 10483.

55 S. Khrapak, B. Klumov and L. Couëdel, *Scientific Reports*, 2017, **7**, 7985.

56 T. Bryk, F. Gorelli, G. Ruocco, M. Santoro and T. Scopigno,

Physical Review E, 2014, **90**, 042301.

57 K. Honda, *Progress of Theoretical Physics*, 1976, **55**, 1024–1037.

This journal is © The Royal Society of Chemistry [year]